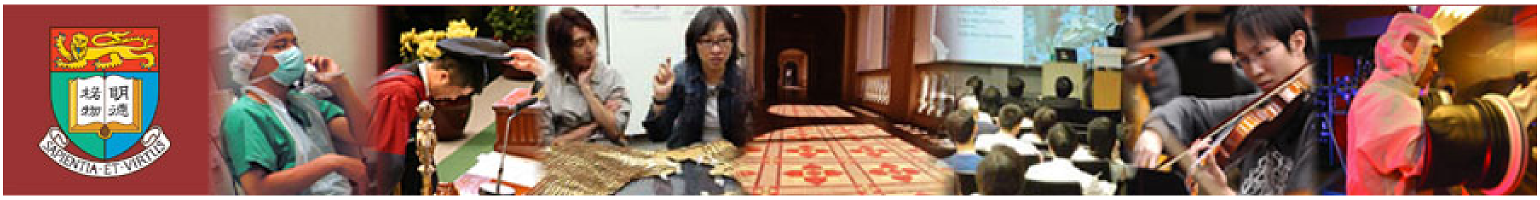

Title	An Extended Photoelectrothermal Theory for LED Systems: A Tutorial From Device Characteristic to System Design for General Lighting
Author(s)	Hui, SYR; Chen, H; Tao, XH
Citation	IEEE Transactions on Power Electronics, 2012, v. 27 n. 11, p. 4571-4583
Issued Date	2012
URL	http://hdl.handle.net/10722/164099
Rights	IEEE Transactions on Power Electronics. Copyright © I E E E.

An Extended Photoelectrothermal Theory for LED Systems: A Tutorial From Device Characteristic to System Design for General Lighting

S. Y. R. Hui, *Fellow, IEEE*, Huanting Chen, and Xuehui Tao

(Invited Paper)

***Abstract*—LED technology is a multidisciplinary subject that involves semiconductor physics, photometry, electric power, heat, and chromaticity. It has been demonstrated that operating the LED load at its rated power does not necessarily guarantee optimal luminous performance unless the LED system is properly designed. This paper presents a tutorial of LED system theory that links the device characteristics to optimal system designs. Based on recent works on the photoelectrothermal theory and its extensions, this paper aims at providing a comprehensive LED system theory with physical explanations for electronics engineers and researchers working in LED system designs, with the emphasis on general and public lighting applications. The physical meanings of essential parameters are explained. Practical test procedures for extracting parameters not readily available in data sheets are included. It is envisaged that this LED system theory will form the basic design guidelines for future LED system designs. This tutorial paper is written not only for educational purpose, but it also highlights important parameters that LED device manufacturers should include in LED data sheets.**

***Index Terms*—Light-emitting diodes, photoelectrothermal theory, solid state lighting.**

I. Introduction

LED is a revolutionary lighting technology that has the potential of replacing energy-inefficient incandescent lamps and mercury-filled fluorescent lamps. Despite its successes in display, decorative, and signaling applications, its applications in general and public lighting are still restricted. There are several major reasons for such limitations in general and public lighting. First, there is still no international standard on the binning systems on color temperature and on the electrical ratings of the LED devices, although an international consortium is working on such standardization [1]. Second, many commercial LED products (i.e., LED systems) failed to meet the manufacturers' claims on the luminous outputs, as recently pointed out in an IET article [2]. Third, the long lifetime enjoyed by LED devices may not be matched by the LED drivers. From a system point of view, the lifetime of the product is determined by the weakest component which has been identified as the electrolytic capacitors [3]–[5] in the driver circuits. These problematic issues are consistent with the conclusions of the panel discussion of the international forum in Shanghai in 2009 [6], which also include eye discomfort caused by the high color temperature (>6000 K) of LEDs involved, vulnerability to lightning and short lifetime of electronic LED drivers, gradual degradation of luminous output as the LED fixtures warm up, and gradual loss of cooling effects of heatsink due to dust deposition and birds' excretion. The significance of the system aspects of the LED technology such as lifetime of LED drivers and thermal designs has been reiterated in recent industrial presentations in [57] and [58]

LEDs with high color temperature tend to have higher luminous efficacy. The imminent requirement of using warm-white LEDs (with lower color temperature) signifies the importance of optimal design of the entire LED system, including the right choice of LED devices, the use of highly reliable LED drivers (preferably with lifetime exceeding 10 years and high robustness against extreme weather conditions such as lightning and wide temperature range), appropriate thermal management [7]–[11], and proper mechanical design of the lighting fixture.

The photometric, electrical, and thermal characteristics of LED systems are highly dependent on one another. This section summarizes some recent research publications that are relevant to these aspects. With increasing demand for higher power density, high-brightness LED is facing challenging thermal problems that affect optical characteristics and reliability [12], [13]. Increasing junction temperature results in the reduction of luminous flux which is known as luminous efficacy droop [14], [15] and such rate of reduction is often measured as a K factor in some semiconductor device literature [16]–[18]. Based on experimental approaches, many researchers have reported findings on such droop characteristics. In [12], the mechanism of the increased nonradiative recombination centers is related to the generation of defects in the active region due to the high current flow through quantum well structure and the increase of LED chip temperature. The effect of temperature on the light output of LED strongly depends on materials and the structure of a chip. It has been reported in [19] that the fundamental origin of the high current "droop" of efficiency observed in LEDs is

Manuscript received August 26, 2011; revised December 4, 2011; accepted February 7, 2012. Date of current version June 20, 2012. This work was supported by the Hong Kong Research Grant Council under Project HKU-114411. Recommended for publication by Associate Editor B. Lehman. (*Invited Tutorial Paper*)

S .Y. R. Hui is with the Departments of Electrical and Electronic Engineering, The University of Hong Kong, Pokfulam, Hong Kong, and also with Imperial College London, London SW7 2AZ, U.K. (e-mail: ronhui@eee.hku.hk).

H. T. Chen is with the Department of Electrical and Electronic Engineering, The University of Hong Kong, Pokfulam, Hong Kong (e-mail: htchen23@yahoo.cn).

X. H. Tao is with the Department of Electronic Engineering, City University of Hong Kong, Kowloon, Hong Kong (e-mail: xuehuitao2@student.cityu.edu.hk).

Color versions of one or more of the figures in this paper are available online at http://ieeexplore.ieee.org.

Digital Object Identifier 10.1109/TPEL.2012.2188648

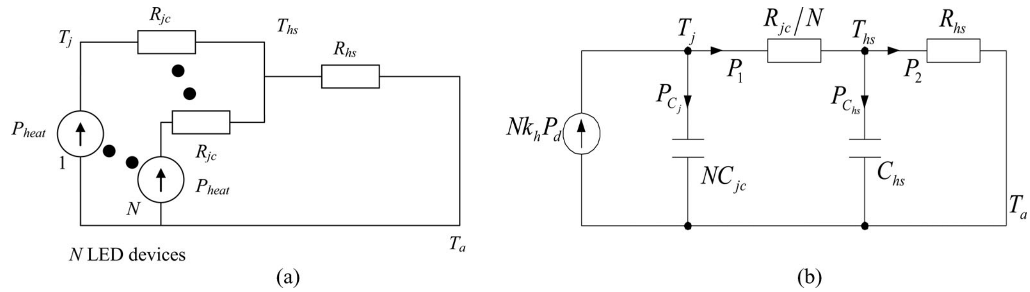

Fig. 1. Simplified steady-state and dynamic thermal equivalent circuits of the LED system with N LEDs mounted on the same heatsink [39], [40]. (a) Steady-state model. (b) Dynamic model.

unlikely caused by incomplete carrier injection or carrier escape but rather is a fundamental material property of LED. Besides the luminous efficacy droop problem, the thermal problem also accelerates aging [20], [21] and causes color shift of LED [22], [23].

Research studies into the theoretical model and parameter extraction are essential in understanding the interactions of heat, light, and power in LED systems. In practice, temperature measurement of LED can be carried out using nematic liquid crystal thermography with laser illumination [24], but such method cannot be used to monitor the junction temperature easily when the LED is housed in a package. A significant advancement was made by Schubert and his team [25] who experimentally established the relationship between the forward voltage V_f and the junction temperature T_j of GaN LED. Such advancement led to similar work for the GaN laser diode [26]. The relationship between T_j and V_f provides a tool for predicting the internal junction temperature which affects luminous efficacy [27], [28], lifetime [20], [21], [29], [30], and color [12], [22], [23], [31]. Based on the structure functions and transient measurement methods, accurate practical thermal measurements for the thermal resistance and capacitance and junction temperature become possible [15]–[17], [55], leading to the development of a commercial LED measurement system [32]. LED researchers have reported electrical modeling of junction temperature prediction in [25]–[27], [33] and thermal resistance [34], [35]. So far, these reports focus on measurements of device parameters and junction temperature without considering overall system design (such as heatsink design) for the optimization of the luminous output. For more accurate studies on the complex interactions of heat, light, and power in LED systems, scientists have to use 3-D finite-element methods [28], [36].

Starting with a brief description of LED device characteristics, this tutorial aims at systematically gathering recent progress in LED system theory and providing sufficient scientific and technological information for electronics engineers and researchers to understand the complex interactions of photometric, electric, thermal, and chromatic aspects of LED systems. It provides an introduction of a comprehensive LED system theory to electronics engineers and researchers for optimal design of LED systems and products. Such system theory offers clear explanations on why LED systems, if not properly designed, may not achieve optimal performance at rated power, and also why their luminous outputs will drop with time. The tutorial also highlights some important features in LED data sheets and their implications and explains nonlinear and interdependent factors affecting LED system performance. Section II will revisit the steady-state and dynamic photoelectrothermal (PET) theories for LED systems, which will be used throughout this paper as the basis for LED system design and optimization. In particular, the physical meanings and determination procedures for important coefficients used in the PET theory for the LED system are included so that LED system designers can understand the physical behavior of the LED devices. The tutorial will point to certain criteria for selecting the design philosophy of LED systems and the optimization design procedure will be addressed in Section III. The implications of the LED system theory on the LED device and system design will be included in Section IV.

II. PET Theory for LED Systems

Assuming that the LED devices are identical and that the heat distribution is even in the heatsink, Fig. 1(a) and (b) shows the simplified steady-state and dynamic thermal equivalent circuits for a general LED system with N LED devices mounted on a heatsink. In practice, heatsink compound or equivalent material may be used between the LEDs and the heatsink to ensure good thermal contact. The thermal resistance of such a thermal compound is smaller than 0.0045 °C-in^2/W [37], [38] and is relatively small when compared with the thermal resistance R_{jc} of LEDs (typically in the order of several °C/Watt) and is neglected in the following analysis.

A. Steady-State PET Theory

The total luminous flux ϕ_v of an LED system consisting of N LED devices can be expressed as

$$\phi_v = N \times E \times P_d \quad (1)$$

where E is the luminous efficacy (lumen/Watt) and P_d is the real power of one LED (W). The LED power is defined as $P_d = V_d \times I_d$, where I_d is the diode current and V_d is the diode voltage. The amount of power dissipated as heat in one LED is defined as

$$P_{\text{heat}} = k_h P_d \quad (2)$$

where k_h is the heat dissipation coefficient that is less than 1.

Among all data provided in the LED data sheet, the luminous efficacy E is one of the most important information that needs thorough understanding. In fact, LED system designers are often power electronics engineers with good knowledge in switched mode power supply design. Consequently, they may inadvertently set the design criterion on maximizing the energy efficiency of the LED driver under the rated power conditions of the LED load. For general and public lighting systems, the top priority should be to maximize the luminous efficacy (lumen/Watt) rather than energy efficiency. Having 100% efficiency without light is meaningless for a lighting system. It must be noted that the typical luminous efficacy value provided in the data sheet is only true at the rated junction temperature which is normally set at 25 °C. As the LED power increases, the junction temperature T_j will also increase. An increase in junction temperature will reduce the luminous efficacy because the LED will emit more phonon (heat) than photons (light) as the wafer temperature increases [14]. The effect of the luminous flux reduction with increasing current has been linked to several mechanisms, such as current leakage by tunneling of electrons to the states of InGaN/GaN interfaces [41], the effects of auger recombination [42], and built-in piezoelectric fields [15].

In the PET theory [39], the relationship of the luminous efficacy and the junction temperature follows the following linear equation as illustrated graphically in LED data sheets:

$$E = E_o\left[1 + k_e\left(T_j - T_o\right)\right] \text{ for } T_j \geq T_o \text{ and } E \geq 0 \qquad (3)$$

where E_o is the rated efficacy at the rated temperature T_o (typically 25 °C in some LED data sheets) and the coefficient k_e is the relative rate of reduction of luminous efficacy with increasing temperature. The luminous efficacy E under discussion in this paper is the one for the LED package only. The optical power loss of the luminaire and the power loss of the LED driver are not included. The parameter k_e is negative because E decreases with increasing T_j.

Based on the steady-state model in Fig. 1(a), the steady-state heatsink temperature T_{hs} can be expressed as

$$T_{hs} = T_a + R_{hs}\left(NP_{\text{heat}}\right) = T_a + R_{hs}\left(Nk_h P_d\right) \qquad (4)$$

where T_a is the ambient temperature. From Fig. 1(a) and (4), the junction temperature of each LED is therefore

$$\begin{aligned} T_j &= T_{hs} + R_{jc}k_h P_d \\ &= T_a + \left(R_{jc} + NR_{hs}\right)k_h P_d. \end{aligned} \qquad (5)$$

Combining (5) and (3) gives the modified luminous efficacy equation as

$$E = E_o\left[1 + k_e\left(T_a - T_o\right) + k_e k_h\left(R_{jc} + NR_{hs}\right)P_d\right]. \qquad (6)$$

The total luminous flux ϕ_v of the LED system according to (1) is

$$\phi_v = NE_o\left\{\left[1 + k_e\left(T_a - T_o\right)\right]P_d + k_e k_h\left(R_{jc} + NR_{hs}\right)P_d^2\right\}. \qquad (7)$$

Equation (7) can be expressed in the form of $\phi_v = \alpha_1 P_d - \alpha_2 P_d^2$ where α_1 and α_2 are positive coefficients. This characteristic equation highlights one important issue, which is easily misunderstood, that increasing the LED power will not always increase the luminous flux output. The luminous flux is roughly proportional to P_d when P_d is small (e.g., less than 1 W) because the second term with P_d^2 is small. As P_d increases and exceeds 1.0, the second term (which is negative) becomes increasingly significant. Consequently, the luminous flux is expected to follow a parabolic curve with a peak value. Beyond the maximum flux operating point, further increase in the LED power will lead to luminous flux drop. This characteristic function of the steady-state PET theory has been practically verified in [39]. Fig. 2(a) and (b) shows the measured and theoretical luminous flux curves and luminous efficacy, respectively, of eight Luxeon K2 Cool-white 3-W LEDs mounted on a heatsink with a thermal resistance of 4.5 °C/W. These results highlight the fact that the luminous flux will drop after the maximum point has been reached and that the luminous efficacy will decrease with increasing LED power.

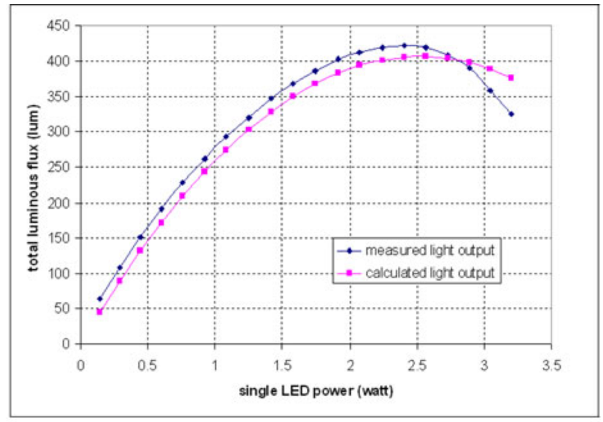

(a)

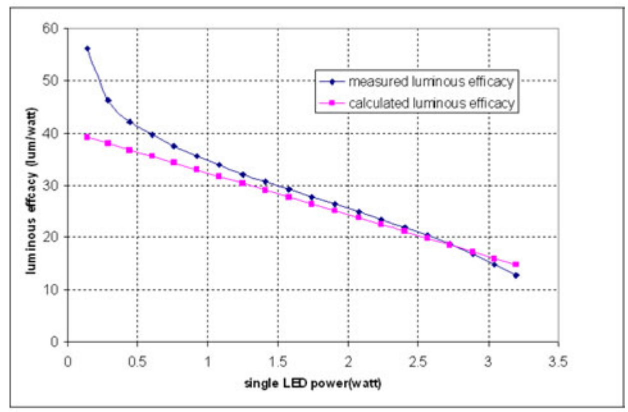

(b)

Fig. 2. (a) Calculated and measured total luminous flux versus lamp power for eight LuxeonK2 Cool-white 3W LEDs mounted on a heatsink with a thermal resistance of 4.5 °C/W [39]. (b) Calculated and measured total luminous efficacy versus lamp power for eight Luxeon K2 Cool-white 3W LEDs mounted on a heatsink with a thermal resistance of 4.5 °C/W [39].

B. Dynamic PET Theory

While (1)–(7) mathematically link up the steady-state relationship of photometric, electrical, and thermal aspects of the LED system based on the model in Fig. 1(a), they do not include the effect of time which is a critical factor, particularly in view of the complaint of the luminous flux decline with time in previous LED system installations. Users of LED systems could also be misled by the high initial luminous flux they see without realizing that the luminous flux level may drop significantly as the heatsink temperature increases gradually. Based on the dynamic model in Fig. 1(b) which includes the thermal capacitance of the LED package and the heatsink, the dynamic PET theory has been developed to incorporate the effect of time. The dynamic and time-dependent versions of (4)–(7) have been shown in [40] to be

$$T_{hs}(t) = \left[\frac{-R_{jc}C_{jc}Nk_hP_dR_{hs}}{C_{jc}R_{jc}-C_{hs}R_{hs}}e^{-t/C_{jc}R_{jc}} + \frac{Nk_hP_dR_{hs}^2C_{hs}}{C_{jc}R_{jc}-C_{hs}R_{hs}}e^{-t/C_{hs}R_{hs}} + NR_{hs}k_hP_d + T_a\right] \quad (8)$$

$$T_j = \left\{-R_{jc}k_hP_d\left(\frac{C_{jc}NR_{hs}}{C_{jc}R_{jc}-C_{hs}R_{hs}}+1\right)e^{-t/C_{jc}R_{jc}} - k_hP_d\left(\frac{-NR_{hs}R_{jc}C_{jc}}{C_{jc}R_{jc}-C_{hs}R_{hs}}+NR_{hs}\right)e^{-t/C_{hs}R_{hs}} + (R_{jc}+NR_{hs})k_hP_d + T_a\right\} \quad (9)$$

$$E = E_o\left[1 + k_e(T_a - T_o) + k_ek_h(R_{jc}+NR_{hs})P_d - k_eR_{jc}k_hP_d\left(\frac{NR_{hs}C_{jc}}{C_{jc}R_{jc}-C_{hs}R_{hs}}+1\right)e^{-t/C_{jc}R_{jc}} + k_ek_hP_d\frac{NR_{hs}^2C_{hs}}{C_{jc}R_{jc}-C_{hs}R_{hs}}e^{-t/C_{hs}R_{hs}}\right] \quad (10)$$

$$\phi_v = NE_o\left\{[1 + k_e(T_a - T_o)]P_d + k_ek_h(R_{jc}+NR_{hs})P_d^2 - k_ek_hR_{jc}\left(\frac{NR_{hs}C_{jc}}{C_{jc}R_{jc}-C_{hs}R_{hs}}+1\right)e^{-t/C_{jc}R_{jc}}P_d^2 + k_ek_h\frac{NR_{hs}^2C_{hs}}{C_{jc}R_{jc}-C_{hs}R_{hs}}e^{-t/C_{hs}R_{hs}}P_d^2\right\} \quad (11)$$

where C_{jc} and C_{hs} are the thermal capacitance of the LED package and the heatsink, respectively, R_{hs} is the heatsink thermal resistance, and t is the time variable.

The dynamic PET theory is important in predicting the luminous flux reduction with time, which is the problem of many commercial LED products as pointed out by the IET article. In (8)–(11), there are two thermal time constants, i.e., $\tau_{jc} = C_{jc}R_{jc}$ for the LED package and $\tau_{hs} = C_{hs}R_{hs}$ for the heatsink. In practice, they are of widely different orders of magnitude. Both thermal time constants are useful to electronics designers. For example, the small thermal time constants are useful in the prediction of the dynamic junction temperature for thermal check (as later described in this paper). The large thermal time constant of the heatsink is useful for predicting the gradual degradation of luminous flux in high power LED systems with relatively large heatsinks. Fig. 3 shows the practical measurements of time-dependent luminous flux of two LED systems based on the same number of LED devices and load power, but mounted on two different heatsinks with different R_{hs}. It can be seen that the luminous flux will reduce significantly when the cooling effect is small (i.e., heatsink size is small or R_{hs} is large). Therefore, this can be a serious problem for LED applications in which space for heatsink is very limited. Examples are LED bulbs for replacing incandescent lamps, and LED headlamps for vehicles. The dynamic theory provides a tool for LED system designers to estimate the luminous flux reduction over time. For continuous operation, the steady-state luminous flux should be checked if it has reached the required level as expected in the technical specification of a general lighting application.

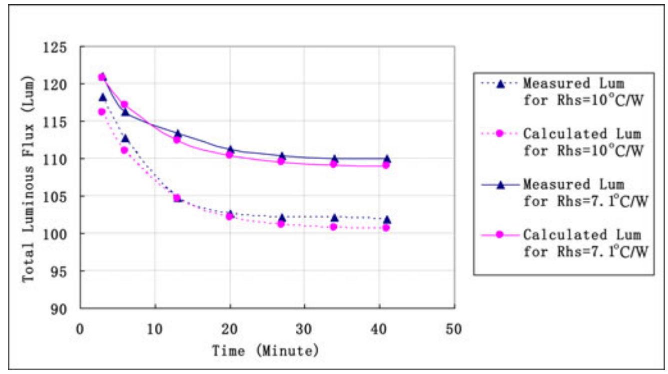

Fig. 3. Variation of the luminous flux with time for eight Luxeon 1-W LEDs operated at rated power [40].

III. Physical Meanings and Determination of Coefficients k_h and k_e

It is important that LED system designers should understand the physical meanings of the coefficients k_h and k_e. In addition, the procedures for their measurements must be simple and practical.

A. Coefficient k_e

The luminous intensity I of LEDs, which is a photometric quantity representing the light intensity of an optical source as perceived by human eyes, decreases with increasing junction temperature. At and near room temperature, the emission intensity follows an exponential decay function [14]

$$I = I|_{25\,^\circ\mathrm{C}} \exp\frac{-(T_j - 25\,^\circ\mathrm{C})}{T_1} \quad (12)$$

where T_1 is the characteristic temperature of the LED. The relationship between the luminous flux ϕ_v and the luminous intensity I is

$$\phi_v = \int I \cdot d\theta \quad (13)$$

where θ is the view angle. The luminous efficacy equation can be expressed as

$$E = \frac{\int I \cdot d\theta}{P_d}. \quad (14)$$

Within the practical range of operating temperature, the reduction of luminous efficacy with increasing junction temperature is fairly linear. It has been mathematically proved [43] that E can be approximated as

$$E = E_o \left[1 - \frac{1}{T_1}(T_j - T_o)\right]. \quad (15)$$

Comparison of (3) and (15) shows that the coefficient k_e used in the PET theory is physically related to the "characteristic temperature" described by semiconductor scientists [14] as

$$k_e = -\frac{1}{T_1}. \quad (16)$$

The coefficient k_e can, therefore, be determined from the characteristic temperature of the LED device. It is also provided in most of the LED data sheets in graphical form.

B. Coefficient k_h

LEDs are not "cool" devices because a significant portion of the LED power consumption will be dissipated as heat [44]. The coefficient k_h in (2) represents the portion of the LED power that is dissipated as heat. It can be measured directly using a "hot-bath" approach in which the LED load is immersed into a bath of silicon oil and the temperature rise is then rated against a predetermined scale of heat loss [44]. This hot-bath approach is very accurate, but is relatively time consuming because each measurement point can only be obtained after the full tank of silicon oil temperature has reached its steady state. Modern LED measurement systems [32] offer a convenient means to obtain thermal, electrical, and optical measurements and parameters for LED devices. With the understanding of its physical meaning, k_h can in fact be related to the optical power and wall-plug efficiency that can be measured by combined thermal and radiometric measurement equipment [32], [53], [54]. Optical measurements of LED samples can be made under thermal and electrical steady-state conditions with the TeraLED system. Once all optical measurements have been performed, the LED is switched OFF and the cooling transient of LED package is monitored with the use of the transient thermal tester (T3Ster). Besides the combined thermal and optical measurements, the temperature dependence of the LED parameters (such as the temperature dependence of the optical power, luminous flux, chromaticity coordinates, and wall-plug efficiency) can also be measured and recorded [55], [56]. LED manufacturers can, therefore, measure and calculate the wall-plug efficiency and then determine the parameter k_h for inclusion in future data sheet

$$k_h = \frac{P_{\rm heat}}{P_d} = \frac{P_d - P_{\rm opt}}{P_d} = 1 - \frac{P_{\rm opt}}{P_d}. \quad (17)$$

The wall-plug efficiency η_w represents the useful portion of the electrical power for light generation and is defined as the ratio of the optical power $P_{\rm opt}$ to the electrical power P_d:

$$\eta_w = \frac{P_{\rm opt}}{P_d}. \quad (18)$$

The optical power $P_{\rm opt}$ is influenced by both the junction temperature T_j and the electrical power P_d. Consequently, η_w is a

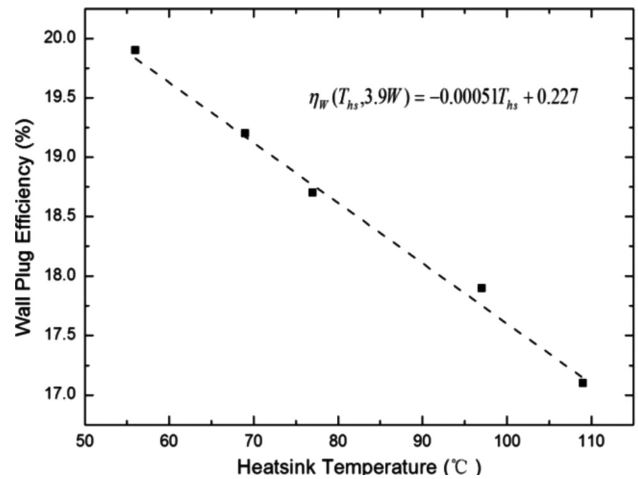

Fig. 4. Typical measured wall-plug efficiency versus heatsink temperature of a sharp 4.4-W LED at constant electrical power [45].

2-D parameter [15], which can be practically determined from the two-test measurement procedures detailed in [45].

In the first test, by fixing P_d at P_o and allowing T_j to vary, the relationship of η_w and T_j at constant P_d ($=P_o$) can be measured and plotted for a Cree LED sample (Model number: XREWHT-L1-0000-007F5) [45]. It can be seen that this is a linear relationship which can be expressed as

$$\eta_w (T_j, P_o) = \alpha T_j + \beta \quad (19)$$

where α and β are the coefficients that can be determined from typical plot using the curve-fitting technique.

Since T_j cannot be monitored directly in an LED system, it is preferable to express (19) in terms of the heatsink temperature T_{hs} which can be measured easily. According to (5) and (17)

$$\begin{aligned}\eta_w (T_j, P_o) &= \alpha T_j + \beta = \alpha[T_{hs} + R_{jc} k_h P_o] + \beta \\ &= \alpha\left[T_{hs} + R_{jc}\left(1 - \frac{P_{\rm opt}}{P_o}\right)P_o\right] + \beta \\ &= \alpha[T_{hs} + R_{jc}(1 - \eta_w)P_o] + \beta. \quad (20)\end{aligned}$$

Rearranging (20) gives

$$\eta_w(T_{hs}, P_o) = \frac{\alpha(T_{hs} + R_{jc}P_o) + \beta}{1 + \alpha P_o R_{jc}}. \quad (21a)$$

Then, at a constant electrical power (P_0), a specific form of $\eta_w(T_{hs}, P_0)$ in (21a) can be rearranged in terms of T_{hs} in the standard form as

$$\eta_w(T_{hs}, P_o) = \sigma T_{hs} + \tau. \quad (21b)$$

As shown in Fig. 4, $\sigma = \alpha/(1 + \alpha P_o R_{jc})$ and $\tau = (\alpha R_{jc} P_o + \beta)/(1 + \alpha P_o R_{jc})$ are fitted coefficients that can be determined from α, β, P_o, and R_{jc} that are known parameters.

In the second test, T_j is kept constant at T_o and P_d is allowed to change. A typical measurement of this test is shown in Fig. 5. It can be seen that this typical curve can be expressed as

$$\eta_w (T_o, P_d) = \chi P_d^2 + \delta P_d + \gamma \quad (22)$$

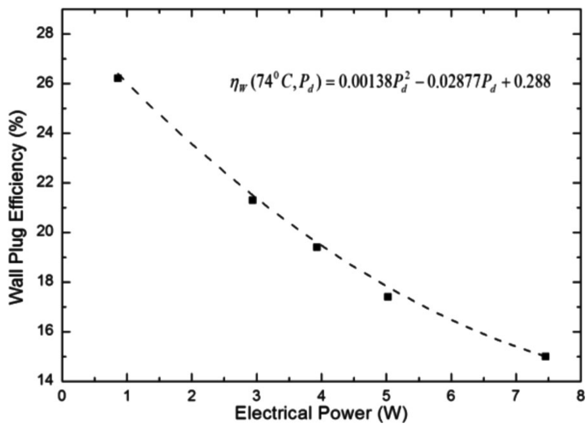

Fig. 5. Typical measured wall-plug efficiency versus electrical power of a sharp 4.4-W LED at constant heatsink temperature [45].

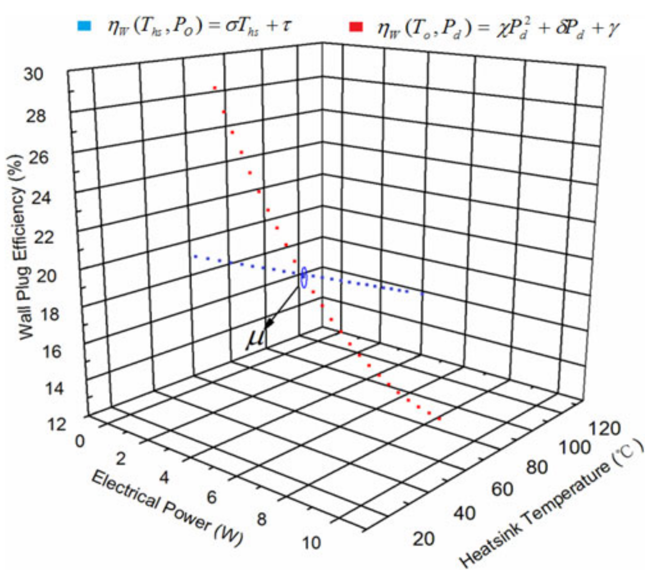

Fig. 6. Wall-plug efficiency of LED as a 2-D function of electrical power and heatsink temperature [45].

where χ, δ, and γ are the coefficients that can be determined from the measured curve using the curve-fitting technique.

After the two-test procedures have been completed and typical curves in Figs. 4 and 5 obtained, these curves can be plotted together as shown in Fig. 6. The intersection point μ of these two curves can then be determined. The general form of η_w can then be expressed as

$$\eta_w(T_{hs}, P_d) = \frac{(\sigma T_{hs} + \tau)\left(\chi P_d^2 + \delta P_d + \gamma\right)}{\mu} = (\sigma' T_{hs} + \tau')(\chi P_d^2 + \delta P_d + \gamma) \quad (23)$$

where μ is the value of the wall-plug efficiency at the intersection point (T_o, P_o), $\sigma' = \sigma/\mu$, and $\tau' = \tau/\mu$.

With the determination of the wall-plug efficiency, according to (17) and (18), the heat dissipation coefficient can be obtained

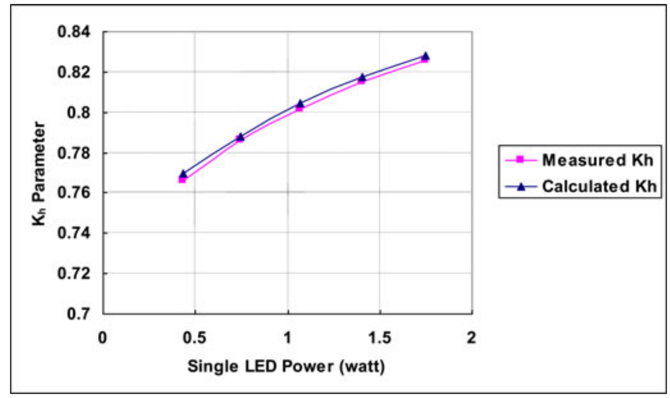

Fig. 7. Measured and calculated k_h parameters versus power.

as

$$k_h = 1 - \frac{P_{\text{opt}}}{P_d} = 1 - \eta_w = 1 - (\sigma' T_{hs} + \tau')(\chi P_d^2 + \delta P_d + \gamma). \quad (24)$$

Let $A = \sigma'(\chi P_d^2 + \delta P_d + \gamma)$ and $B = \tau'(\chi P_d^2 + \delta P_d + \gamma)$; then k_h becomes

$$k_h = 1 - AT_{hs} - B. \quad (25)$$

Fig. 7 shows typical measurement and theoretical prediction of k_h for the same LED sample. It can be seen that k_h varies with P_d.

IV. Applications of the Extended PET Theory for LED System Design

The choice of using the steady-state or dynamic PET theory depends on the nature of the applications (i.e., whether the operation is momentary or continuous). For LED systems that are operated in a momentary manner, such as traffic lights or vehicle signal lights, the dynamic (8)–(11) are appropriate. For example, the red, amber, and green lights of a traffic light have different turn-on times. Theoretically speaking, their optimal heatsink designs could be different. However, since most of the general and public lighting systems require continuous operation, the following discussion is based on the steady-state PET theory.

A. Effect of LED Power on Luminous Flux and Choice of Operating Point

Equation (9) follows the form $\phi_v = \alpha_1 P_d - \alpha_2 P_d^2$, which is a parabolic curve. The maximum value of ϕ_v occurs at a specific LED power P_d^*, which can be expressed as [39]

$$P_d^* = -\frac{[1 + k_e(T_a - T_o)]}{2k_e k_h (R_{jc} + NR_{hs})}. \quad (26)$$

The parameter k_e of (16) is negative. Therefore, the negative sign of the term on the right-hand side makes the whole term positive. In [39], eight identical white LEDs with rated power of 3 W are tested with three different heatsinks (and three different R_{hs} values). The luminous flux measurements with power variation

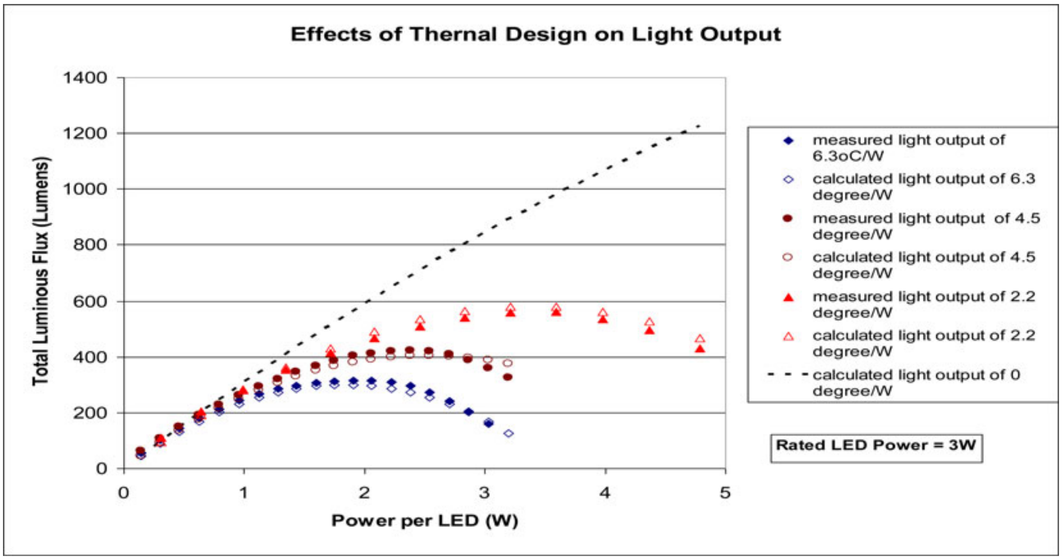

Fig. 8. Luminous flux curves of eight identical LEDs (rated at 3 W) mounted on three heatsinks with different thermal resistance R_{hs} [39].

are shown in Fig. 8. It is of paramount importance to note the fact that the maximum ϕ_v does not necessarily occur at the rated power. In the first curve with the largest R_{hs}, the maximum ϕ_v occurs at about 2 W, meaning that operating this particular LED system at a lower power will generate higher luminous flux. LED system designers with power supply experience must understand the meaning of (26). Otherwise, powering the LED system at the rated power will only result in power wastage and reduction of luminous efficacy and luminous output. The implications of the parameters in the denominator of (26) should be carefully considered.

Several considerations should be included in the choice of the operating point.

1) Equations (7) and (26) can be used together to plot a range of luminous flux for a range of heatsink thermal resistance. This allows the designer to choose the size of the heatsink and the number of LED devices in order to meet the steady-state luminous flux requirement within the constraints of the given size of the heatsink.
2) The choice of P_d^* must not exceed but needs not be the same as the rated LED power. A choice of P_d^* at 80% of the rated power, for example, can lengthen the lifetime of the LED devices and improve the luminous efficacy as the LEDs are operated at a reduced junction temperature.

B. Effects of the Heatsink Thermal Resistance R_{hs}

The results in Fig. 8 indicate that increasing the cooling effect of the heatsink (i.e., with a lower R_{hs}) can shift the maximum ϕ_v operating point to the right (at a higher P_d). This means that the thermal design and the choice of the heatsink or other cooling methods are critical in the optimization of the LED system. Good thermal design enables the heat generated in the LED wafer to be extracted out of the junction. A lower junction temperature leads to a higher luminous efficacy as implied by (3). The choice of the heatsink, however, depends on the applications [46].

1) For applications in which the size available for heatsink is restricted (as in the case of curve-1 in Fig. 8), operating the LED at a power lower than the rated power may even generate more light than at the rated power.
2) For applications in which the size available for the heatsink is less restrictive, the theoretical P_d* point can be set at a value higher than the rated power. The system should then be operated at the rated power in order to maximize the luminous flux output without reducing the lifetime of the LEDs.

C. Effects of LED Package Thermal Resistance R_{jc}

The thermal resistance of the LED is an important factor that LED system designers should consider. A large R_{jc} will reduce the heat flow from the junction to the case and thus lead to a high junction temperature, which in turn reduces the luminous efficacy. For example, a 5-W LED with R_{jc} of 10 °C/W will have a temperature difference of 50 °C between the junction and the case alone. So, LED system designers should choose LED with R_{jc} as small as possible.

In the commercial LED market, there are single-chip and multichip structures for white LEDs. In general, multichip structures have lower R_{jc} because R_{jc} of individual wafers are paralleled. For the same device power, it has been shown in [47] that LED with multichip structure has a lower R_{jc} and higher ϕ_v than LED with a single-chip structure. A typical comparison of single-chip (CREE X lamp XR-E series 3-W LED device) and multichip (Sharp GW5 C15L00 3-W LED device) LED structures is shown in Fig. 9 [47].

D. Effects of the Number of LED Devices N

An important issue that LED system designers should consider is whether one should use several LEDs of smaller rated power or one LED with higher rated power. Based on the same parallel principle for reducing the overall thermal resistance, it

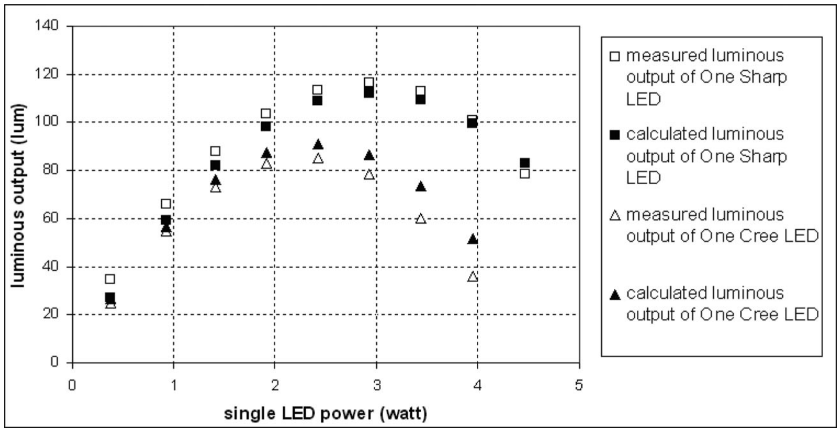

Fig. 9. Measured and calculated luminous output of comparison between one SHARP and one CREE LED with the same total power on the separate heatsinks with the same thermal resistance 30 °C/W [47].

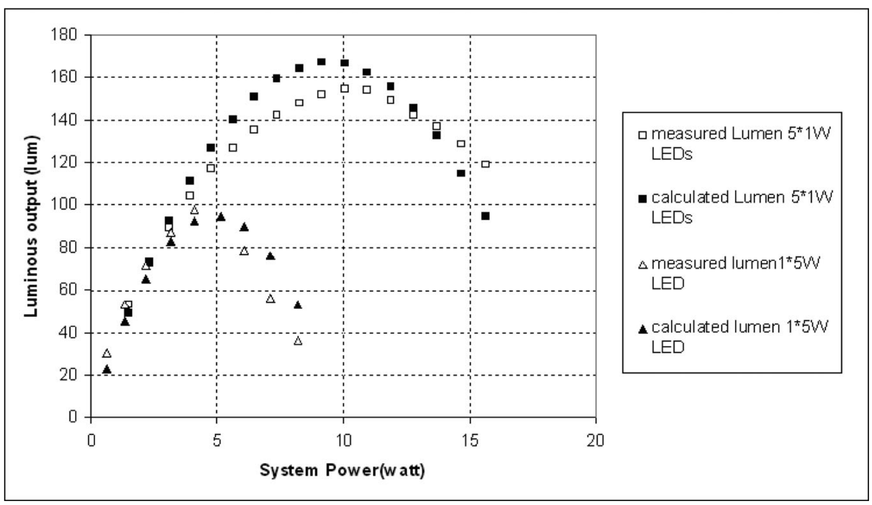

Fig. 10. Measured and calculated luminous output of an LED system with one 5-W LED and a system with five 1-W LEDs using the same type of heatsinks with the same thermal resistance 8.5 °C/W [47].

has been demonstrated [47] that, for the same overall power output, using more LEDs with lower rated power provides more contact area for heat transfer than using less LEDs with higher rated power. Fig. 10 shows typical comparison of using five LEDs of 1 W and one LED of 5 W. The use of LEDs in parallel can always increase the contact area and reduce the effective thermal resistance that facilitates heat removal from the junction.

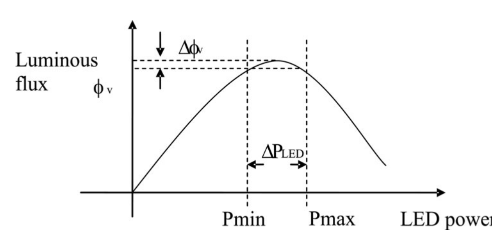

Fig. 11. Example of reducing luminous flux variation using the top region of the flux-power curve [48].

E. Effects of the Parabolic Curve of the Luminous Flux Against LED Power

1) Use of Top Region of the Curve for Reducing Sensitivity of Luminous Flux Variation: The parabolic curve of the luminous flux versus LED power in Fig. 8 opens a new opportunity to design the LED system with minimum luminous flux fluctuation. The slope of the parabolic curve at and around the peak value is relatively small. If the LED power is controlled within the specified range as indicated in Fig. 11, the variation of the luminous flux is minimal. This is an important and unique feature of the LED system that differentiates LED from other general lighting systems such as the high-intensity-discharge (HID) lamps that are commonly used in road lighting systems.

The top part of the parabolic curve is a useful region for designing large-scale public lighting systems as a new generation of smart loads for future smart grid with substantial penetration of intermittent renewable energy sources. The increasing use of dynamically changing renewable power sources will unavoidably introduce instability to future power grids. Properly designed LED systems can cope with wide fluctuation in mains voltage. An example of a smart LED system of 130 W based on

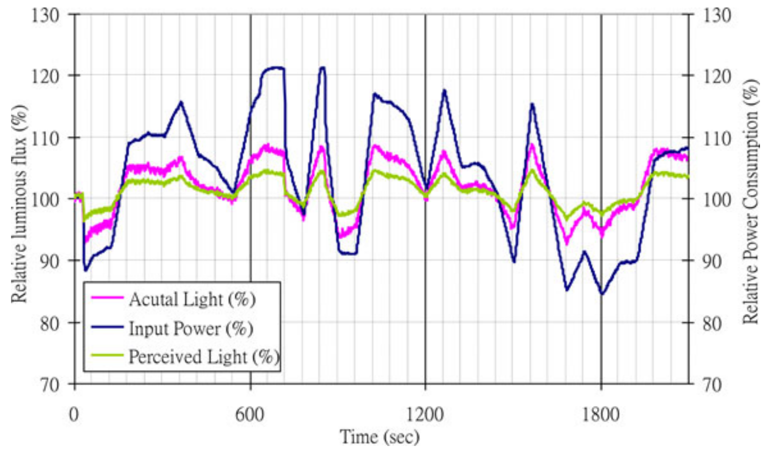

Fig. 12. Measured input power, actual light, and perceived light of the LED lighting system under a weakly regulated renewable power grid [48].

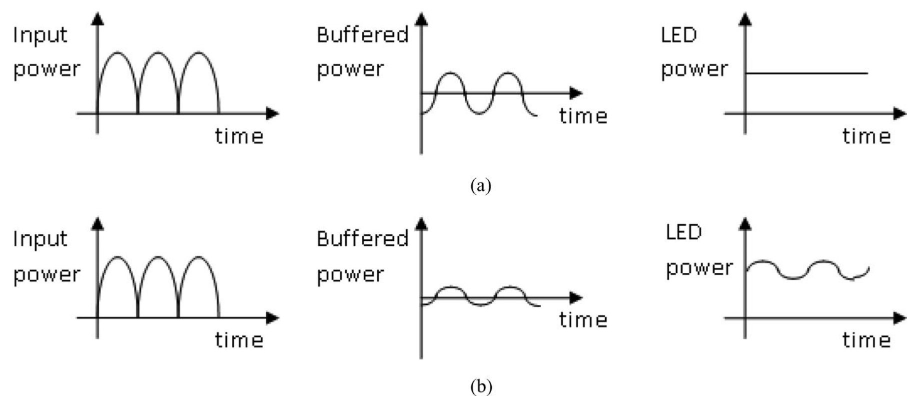

Fig. 13. Power profiles of a typical offline LED lighting system (a) with tightly regulated output power and (b) with power output with fluctuation.

this design principle [48], [49] is shown in Fig. 12. In this example, a variation of 40 V in the mains voltage will lead to only 15% of luminous flux variation, as compared to 40% luminous flux variation in existing HID lamp systems.

2) Use of Top Region of the Curve for Reducing Energy Storage and Elimination of Electrolytic Capacitors in LED Drivers: The possibility of allowing LED power to change within a certain power range implies that there is no need to use switched mode power supply as LED driver to tightly regulate the LED power. This principle [48], [49] is illustrated in Fig. 13. For an offline LED system fed by ac mains, the input power of the system is pulsating. If the LED power is allowed to fluctuate, the energy storage requirement of the LED driver can be significantly reduced. This important feature indicates that an electrolytic capacitor can be eliminated in LED driver design if the LED power is allowed to vary, as explained previously.

1) For compact LED driver design, electronic LED drivers without electrolytic capacitors have been proposed [3]–[5], [13], [50], [51]. However, the theory enables system designers to use traditional switched mode power circuits without tight current output regulation (see Fig. 14) to drive the LED load. A comparison of existing methods and the proposed method is tabulated in Table I.
2) For an LED driver with less restriction on size and volume such as road lighting system where the lamp posts provide ample space, passive LED drivers (see Fig. 15) without active power switches, control integrated circuits, and auxiliary power supply, and with low component counts, high efficiency and reliability, and robustness against extreme weather conditions can be used [49], [52].

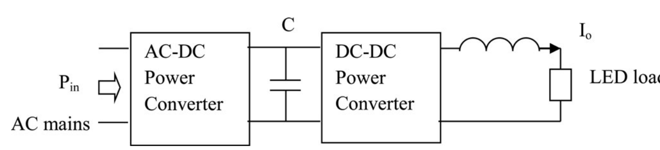

Fig. 14. General schematic of an offline passive or active LED driver with a current source output.

TABLE I
COMPARISON OF EXISTING AND PROPOSAL METHODS

	Existing Method 1 (Constant output power)	Existing Method 2 (Pulsating output power)	Proposed Method (Output current with limited variation)
Output current	Constant 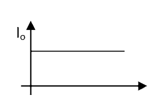	large power variation with *zero power points* 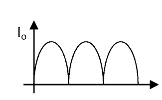	Limited power variation with *continuous non-zero minimum current* 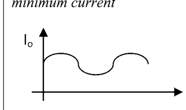
Energy Storage requirement:	Large electrolytic capacitor is needed.	Electrolytic capacitor is not needed.	Electrolytic capacitor is not needed.
Flickering effects	No (no power variation)	Yes (large power variation with zero power points)	No (restricted power variation with a strong minimum power)

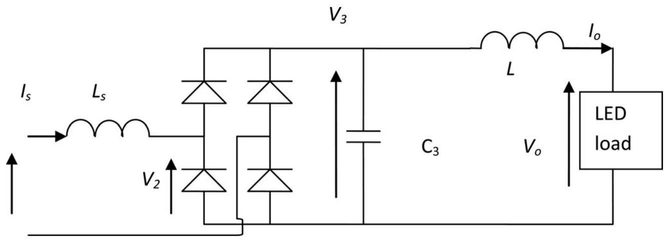

Fig. 15. Example of a passive offline LED driver for general lighting [49].

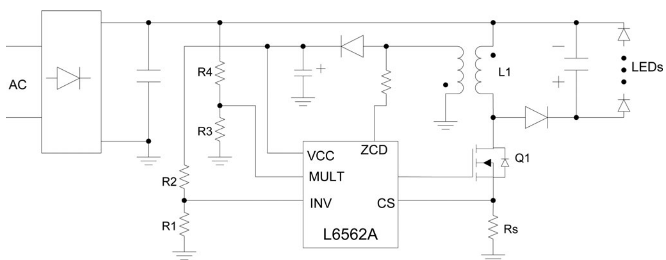

Fig. 16. Offline LED system provided by ST Microelectronics.

TABLE II
LED System Parameters

k_e	E_o	T_a	T_o	N	R_{jc}	R_{hs}	$\tau_{LED} = C_{jc}R_{jc}$	$\tau_{hs} = C_{hs}R_{hs}$
-0.003	58	28	25	18	8.5	4.1	0.7	380

F. Use of a Dynamic Model for Photometric and Thermal Performance Checks

So far, explanations have been given to guide LED system designers to choose the parameters based on the steady-state model. Once the LED driver is chosen, it is imperative to use the dynamic model for photometric and thermal checks. The idea is to ensure that the LED system will provide sufficient luminous flux to meet the required specification and that the instantaneous junction temperature will not exceed the maximum temperature rating stipulated in the manufacturers' data sheets.

The output power (as a function of time) of the LED driver can be used as the input of the model. This time-domain output power function of the LED driver can be obtained either from circuit simulation of the LED system or practical measurements from a hardware prototype. The driving function for the dynamic model shown in Fig. 1(b) is $Nk_h P_d(t)$. The junction temperature T_j and the luminous flux ϕ_v can then be predicted as a function of time.

The dynamic modeling of an offline LED system is used as an example here. Fig. 16 shows the schematic of a typical offline LED driver with an LED load. A ST Microelectronic L6562A evaluation board is used to drive the LED load so that practical measurements can be obtained for comparison with the computed results obtained from the proposal dynamic model. The load consists of 18 CREE 1-W LEDs. The parameters for this setup are tabulated in Table II. The output power of the LED driver is shown in Fig. 17, which can be used as the input (i.e., NP_d) for the equivalent circuit in Fig. 1(b). The parameter k_h is given in Fig. 7.

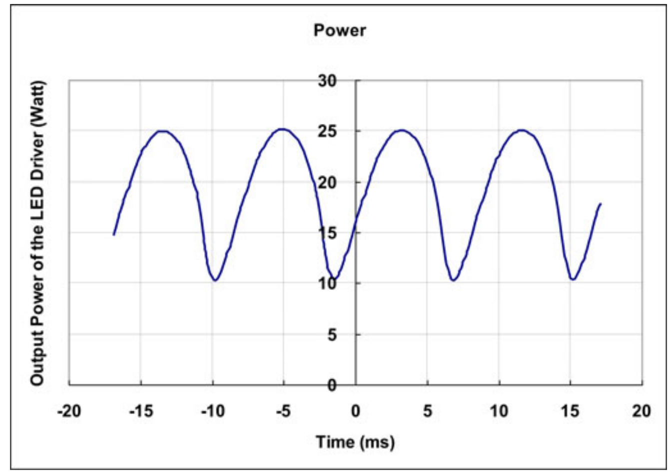

Fig. 17. Waveform of the input power to the LED load.

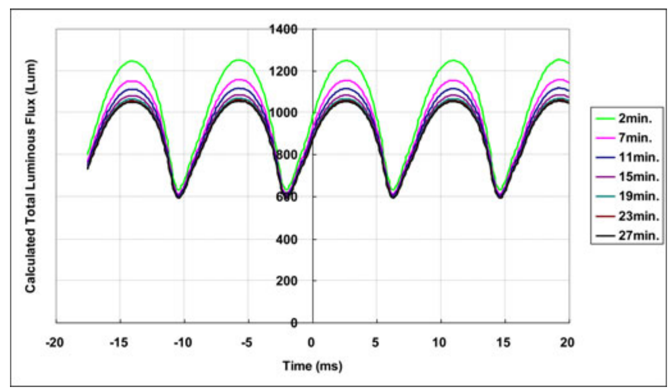

Fig. 18. Predicted luminous flux of an offline LED system at different intervals after turning on the system.

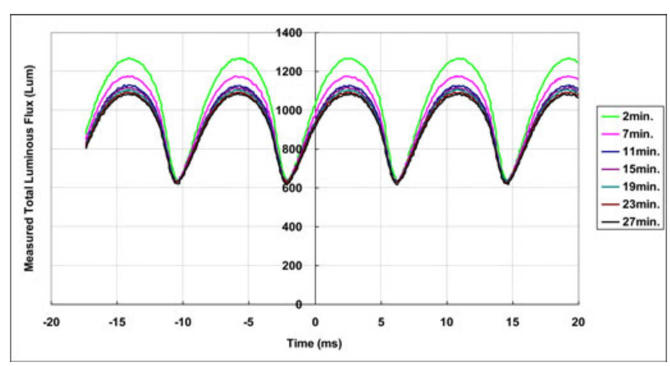

Fig. 19. Measured luminous flux of an offline LED system at different intervals after turning on the system.

Figs. 18 and 19 show the predicted and measured luminous flux variations, respectively, recorded at different intervals after the system has been turned ON. The good agreement confirms the usefulness of this design tool. The corresponding predicted T_j variation is plotted in Fig. 20. It can be seen that T_j increases with time (as the heatsink warms up). Consequently, ϕ_v decreases with time. If the peak T_j value exceeds the maximum temperature allowed, the thermal design has to be adjusted so as to reduce the peak T_j value below its maximum allowable value.

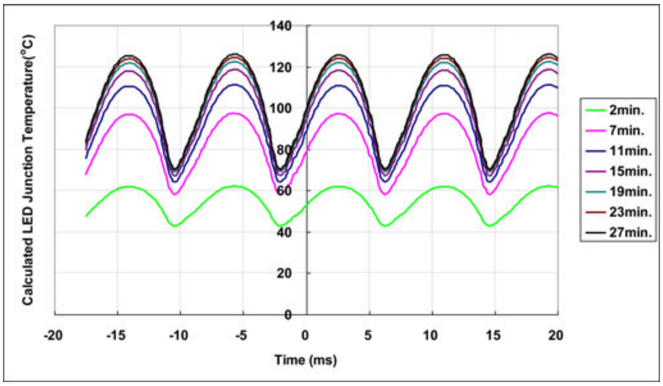

Fig. 20. Predicted LED junction temperature of an offline LED system at different intervals after turning on the system.

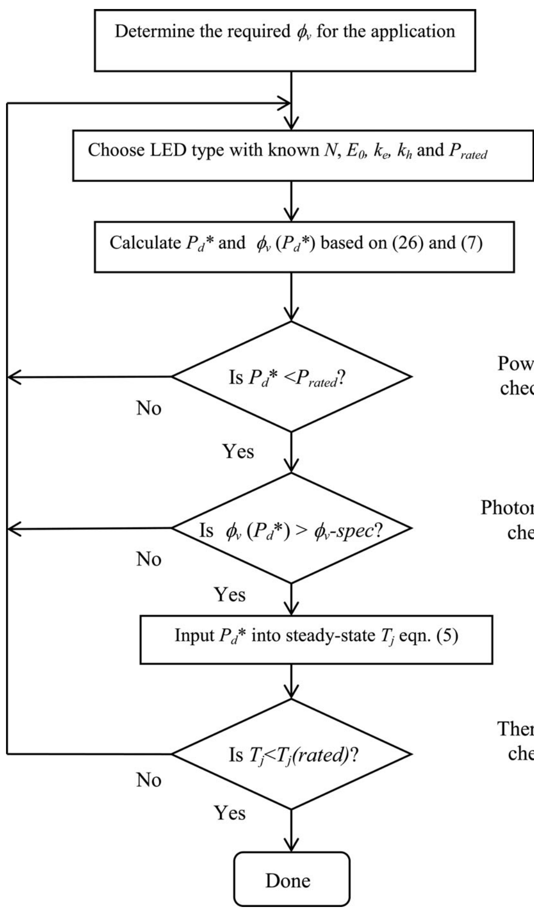

Fig. 21. Flowchart of the design procedure of an LED system with continuous operation, constant power, and a heatsink with limited size.

Engineers can, therefore, use the dynamic model for the photometric and thermal checks, and fine-tuning the LED system design.

G. Flowcharts for System Design Examples

Different LED products and systems have different design philosophies and objectives. It is difficult to use one single design procedure to govern all LED system designs. Here, two examples are illustrated with the use of the extended PET theory. The first design assumes continuous operation of an LED system with load power kept constant by an LED driver and the volume available for the heatsink is limited. Fig. 21 shows the flowchart of the design procedure. Due to continuous operation, the steady-state model and equations are used. For a limited and given heatsink size, the optimal power for the maximum luminous output may not occur at the rated power of the LEDs. It should be highlighted that power, photometric, and thermal checks should be carried out. These three performance checks are essential for all LED system designs.

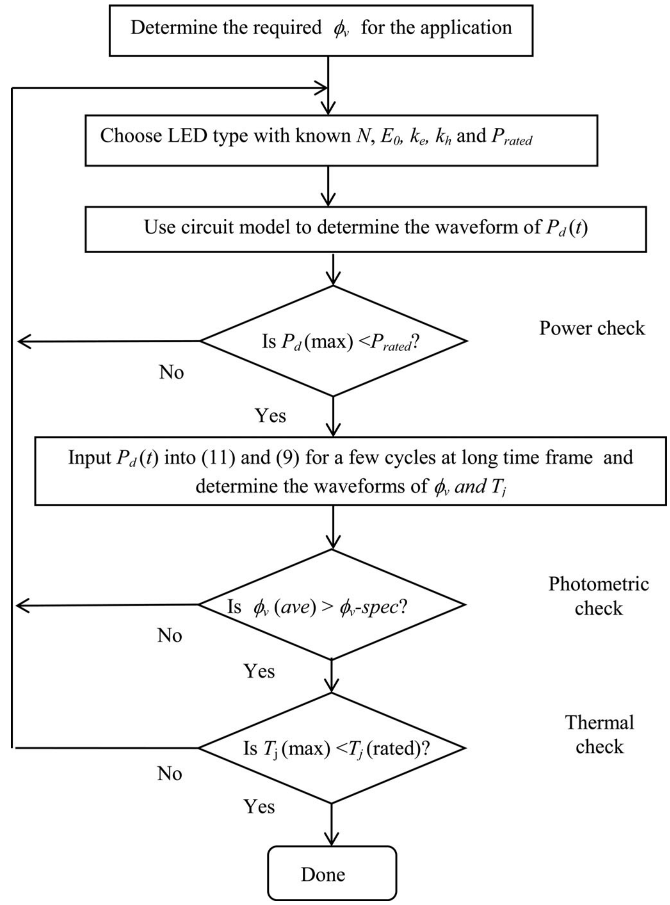

Fig. 22. Flowchart of the design procedure of an offline LED system with continuous operation and fluctuating power.

The same principles apply to the second example of an offline LED system in which the load power is not kept constant. The flowchart is shown in Fig. 22. Due to the variation of LED power, the dynamic model and equations should be used. For applications in which the load power can vary, it is important to check the waveforms of power, luminous flux, and junction temperature. It is preferable to ensure that 1) the peak power does not exceed the rated power; 2) the average luminous flux meets the system specification; and 3) the peak junction temperature does not exceed the rated junction temperature.

V. Conclusion

This paper provides a tutorial on LED system theory based on the extended PET theory. Starting with the device characteristic, it provides the photometric, electrical, and thermal equations and explanations necessary for LED system design. The parameters involved in the theory are derived and their physical meanings are explained. Practical procedures for extracting the parameters not available from data sheets are included. The use of the theory for system design and their implications are substantiated with practical results recently reported in various references. Finally, the implications of the PET theory for the choice of LED devices, heatsink, and LED driver designs are explained. The extended PET theory also highlights several unique features of LED systems that differentiate them from switched mode supplies. This tutorial provides the necessary materials for electronics engineers with switched mode power supply design background for optimal LED system designs. Present LED data sheets do not contain all the parameters described in this theory. It is suggested that these parameters, such as k_h, k_e, and the thermal time constant of the LED package, will be included in future LED data sheets as useful information for LED system designers.

ACKNOWLEDGMENT

The authors would like to thank Dr. C. K. Lee, Dr. W. Chen, S. Li, and W. M. Ng for their research collaboration on various projects based on which this tutorial paper is prepared. S. Y. Hui acknowledges the constructive technical discussion with Dr. J. Shao of ST Microelectronics on the dynamic junction temperature issues.

REFERENCES

[1] [Online]. Available: http://www.zhagastandard.org/2012

[2] M. Harris, "Let there be light," *IET (E&T) Mag.*, vol. 4, no. 20, pp. 18–21, Nov. 2009.

[3] B. Wang, X. Ruan, K. Yao, and M. Xu, "A method of reducing the peak-to-average ratio of LED current for electrolytic capacitor-less AC–DC drivers," *IEEE Trans. Power Electron.*, vol. 25, no. 3, pp. 592–601, Mar. 2010.

[4] L. Gu, X. Ruan, M. Xu, and K. Yao, "Means of eliminating electrolytic capacitor in AC/DC power supplies for LED lightings," *IEEE Trans. Power Electron.*, vol. 24, no. 5, pp. 1399–1408, May 2009.

[5] Y. X. Qin, H. S. H. Chung, D. Y. Lin, and S. Y. R. Hui, "Current source ballast for high power lighting emitting diodes without electrolytic capacitor," in *Proc. IEEE Ind. Electron.*, Orlando, FL, Nov. 2008, pp. 1968–1973.

[6] Panel discussion at the 3rd China International Forum on Novel Light and Energy Sources, Shanghai, China, Apr. 2009.

[7] J. H. Cheng, C. K. Liu, Y. L. Chao, and R. M. Tain, "Cooling performance of silicon-based thermoelectric device on high power LED," in *Proc. 24th Int. Conf. Thermoelectrics*, Clemson, SC, Jun. 2005, pp. 53–56.

[8] J. M. Zhou and W. Yan, "Experimental investigation on the performance and characteristics of white LEDs used in illumination application," in *Proc. IEEE Power Electron. Spec. Conf.*, Orlando, FL, Jun. 2007, pp. 1436–1440.

[9] T. Zahner, "Thermal management and thermal resistance of high power LEDs," in *Proc. 13th Int. Workshop on Thermal Investigation ICs and Syst.*, Budapest, Hungary, Sep. 2007, pp. 195–195.

[10] L. Yuan, S. Liu, M. X. Chen, and X. B. Luo, "Thermal analysis of high power LED array packaging with microchannel cooler," in *Proc. 7th Int. Conf. Electron. Packag. Technol.*, Shanghai, China, Aug.2006, pp. 1–5.

[11] C. Biber, "LED light emission as a function of thermal conditions," *IEEE Semicond. Thermal Meas. Manage. Symp.*, San Jose, CA, Mar. 2008, pp. 180–184.

[12] A. Uddin, A. C. Wei, and T. G. Andersson, "Study of degradation mechanism of blue light emitting diodes," *Thin Solid Films*, vol. 483, no. 1–2, pp. 378–381, Jul. 2005.

[13] X. Ruan, B. Wang, K. Yao, and S. Wang, "Optimum injected current harmonics to minimize peak-to-average ratio of LED current for electrolytic capacitor-less AC–DC drivers," *IEEE Trans. Power. Electron.*, vol. 26, no. 7, pp. 1820–1825, Jul. 2011.

[14] E. F. Schubert, *Light-Emitting Diodes*, 2nd ed. Cambridge, U.K.: Cambridge Univ. Press, 2006.

[15] M. H. Kim, M. F. Schubert, Q. Dai, J. K. Kim, E. F. Schubert, J. Piprek, and Y. Park, "Origin of efficiency droop in GaN-based light-emitting diodes," *Appl. Phys. Lett.*, vol. 91, no. 18, p. 183507 (1)–(3), Oct. 2007.

[16] A. Poppe, Y. Zhang, J. Wilson, G. Farkas, P. Szabó, J. Parry, M. Rencz, and V. Székely, "Thermal measurement and modeling of multi-die packages," *IEEE Trans. Compon. Packag. Technol.*, vol. 32, no. 2, pp. 484–492, Jun. 2009.

[17] G. Farkas, Q. V. V. Vader, A. Poppe, and G. Bognár, "Thermal investigation of high power optical devices by transient testing," *IEEE Trans. Compon. Packag. Technol.*, vol. 28, no. 1, pp. 45–50, Mar. 2005.

[18] M. Rencz, A. Poppe, E. Kollar, S. Ress, and V. Székely, "Increasing the accuracy ofstructure function based thermal material parameter measurements," *IEEE Trans. Compon. Packag. Technol.*, vol. 28, no. 1, pp. 51–57, Mar. 2005.

[19] A. Laubsch, M. Sabathil, J. Baur, M. Peter, and B. Hahn, "High-power and high-efficiency InGaN-based light emitters," *IEEE Trans. Electron. Devices*, vol. 57, no. 1, pp. 79–87, Jan. 2010.

[20] L. Trevisanello, M. Meneghini, G. Mura, M. Vanzi, M. Pavesi, and G. Meneghesso, "Accelerated life test of high brightness light emitting diodes," *IEEE Trans. Device Mater. Reliab.*, vol. 8, no. 2, pp. 304–311, Jun. 2008.

[21] N. Narendran and Y. Gu, "Life of LED-based white light sources," *IEEE/OSA J. Display Technol.*, vol. 1, no. 1, pp. 167–171, Sep. 2005.

[22] S. Chhajed, Y. Xi, Y. L. Li, T. Gessmann, and E. F. Schubert, "Influence of junction temperature on chromaticity and color-rendering properties of trichromatic white-light sources based on light-emitting diodes," *J. Appl. Phys.*, vol. 97, no. 5, p. 054506 (1)–(8), Sep. 2005.

[23] A. Keppens, W. R. Ryckaert, G. Deconinck, and P. Hanselaer, "Modeling of high power light-emitting diode spectra and their variation with junction temperature," *J. Appl. Phys.*, vol. 108, no. 4, p. 043104 (1)–(7), Sep. 2010.

[24] C. Y. Lee and J. Park, "Temperature measurement of visible light-emitting diodes using nematic liquid crystal thermography with laser illumination," *IEEE Photon. Technol. Lett.*, vol. 9, no. 7, pp. 5068–5075, Jul. 2009.

[25] Y. Xi and E. F. Schubert, "Junction-temperature measurement in GaN ultraviolet light-emitting diodes using diode forward voltage method," *Appl. Phys. Lett.*, vol. 85, no. 12, pp. 2163–2165, Jun. 2009.

[26] Y. T. Liu, Q. Cao, G. F. Song, and L. H. Chen, "The junction temperature and forward voltage relationship of GaN-based laser diode," *Laser Phys.*, vol. 19, no. 3, pp. 400–402, 2009.

[27] J. Park and C. C. Lee, "An electrical model with junction temperature for LEDs and the impact on conversion efficiency," *IEEE Electron. Device Lett.*, vol. 26, no. 5, pp. 308–310, May 2005.

[28] W. H. Chi, T. L. Chou, C. N. Han, S. Y. Yang, and K. N. Chiang, "Analysis of thermal and luminous performance of MR-16 LED lighting module," *IEEE Trans. Compon. Packag. Technol.*, vol. 33, no. 4, pp. 713–721, Dec. 2010.

[29] O. Pursiainen, N. Linder, A. Jaeger, R. Oberschmid, and K. Streubel, "Identification of aging mechanisms in the optical and electrical characteristics of light-emitting diodes," *Appl. Phys. Lett.*, vol. 78, no. 18, pp. 2895–2897, Oct. 2002.

[30] N. Narendran and E. Hong, "A method for projecting useful life of LED lighting systems," *Proc. SPIE*, vol. 5187, pp. 93–99, 2004.

[31] P. Manninen and P. Orreveteläinen, "On spectral and thermal behaviors of AlGaInP light-emitting diodes under pulse-width modulation," *Appl. Phys. Lett.*, vol. 91, no. 18, p. 181121 (1)–(3), Oct. 2007.

[32] Mentor Graphics, "Thermal transient tester technical information," [Online]. Available: https://www.mentor.com/products/mechanical/products/upload/t3ster-technical-info.pdf,2011

[33] Y. J. Lee, C. J. Lee, and C. H. Chen, "Determination of junction temperature in InGaN and AlGaInP light-emitting diodes," *IEEE J. Quantum Electron.*, vol. 46, no. 10, pp. 1450–1455, Oct. 2010.

[34] P. Szabo, O. Steffens, M. Lenz, and G. Farkas, "Transient junction-to-case thermal resistance measurement methodology of high accuracy and repeatability," *IEEE Trans. Compon. Packag. Technol.*, vol. 28, no. 4, pp. 630–636, Dec. 2005.

[35] R. H. Horng, J. S. Hong, Y. L. Tsai, D. S. Wu, C. M. Chen, and C. J. Chen, "Optimized thermal management from a chip to a heat sink for high-power GaN-based light-emitting diodes," *IEEE Trans. Electron Devices*, vol. 57, no. 9, pp. 2203–2207, Sep. 2010.

[36] S. Huang, H. Wu, B. Fan, B. Zhang, and G. Wang, "A chip-level electrothermal-coupled design model for high-power light-emitting diodes," *J. Appl. Phys.*, vol. 107, no. 5, p. 054509 (1)–(8), Mar. 2010.
[37] HERNON Dissipator 746, "High performance adhesives and sealant," Technical Data Sheet, [Online]. Available: http://www.hernonmfg.com, 2009, 2012.
[38] (2011). [Online]. Available: http://www.arcticsilver.com/as5.htm
[39] S. Y. R. Hui and Y. X. Qin, "A general photo-electro-thermal theory for light-emitting-diode (LED) systems," *IEEE Trans. Power Electron.*, vol. 24, no. 8, pp. 1967–1976, Aug. 2009.
[40] X. H. Tao and S. Y. R. Hui, "Dynamic photoelectrothermal theory for LED systems," *IEEE Trans. Ind. Electron.*, vol. 59, no. 4, pp. 1751–1759, Apr. 2012.
[41] N. I. Bochkareva, E. A. Zhirnov, A. A. Efremov, Y. T. Rebane, R. I. Gorbunov, and Y. G. Shreter, "Tunnel-recombination currents and electroluminescence efficiency in InGaN/GaN LEDs," *Semiconductors*, vol. 39, no. 5, pp. 594–599, May 2005.
[42] Y. C. Shen, G. O. Mueller, S. Watanabe, N. F. Gardner, A. Munkholm, and M. R. Krames, "Auger recombination in InGaN measured by photoluminescence," *Appl. Phys. Lett.*, vol. 91, no. 14, p. 141101 (1)–(3), Oct. 2007.
[43] X. H. Tao, H. T. Chen, and S. Y. R. Hui, "A new non-contact measurement method for predicting both internal junction temperature and thermal resistance in LED systems," *IEEE Trans. Power Electron*, vol. 27, no. 4, pp. 2184–2192, Apr. 2012.
[44] Y. X. Qin, D. Y. Lin, and S. Y. R. Hui, "A simple method for comparative study on the thermal performance of light emitting diodes (LED) and fluorescent lamps," *IEEE Trans. Power Electron.*, vol. 24, no. 7, pp. 1811–1818, Jul. 2009.
[45] H. T. Chen, X. H. Tao, and S. Y. R. Hui, "Estimation of optical power and heat dissipation coefficient for the photo-electro-thermal theory for LED systems," *IEEE Trans. Power Electron*, vol. 27, no. 4, pp. 2176–2183, Apr. 2012.
[46] S. Y. R. Hui, "Methods for optimal operation of light emitting diodes", U.S. Patent application, 12/370101, Feb. 13, 2009.
[47] Y. X. Qin and S. Y. R. Hui, "Comparative study on thestructural designs of LED devices and systems based on the general photo-electro-thermal theory," *IEEE Trans. Power Electron.*, vol. 25, no. 2, pp. 507–513, Feb. 2010.
[48] C. K. Lee and S. Y. R. Hui, "A design methodology for smart LED lighting systems driven by weakly-regulated power grids," *IEEE Trans. Smart Grid.*, vol. 2, no. 3, pp. 548–554, Sep. 2011.
[49] S. Y. R. Hui and W. Chen, "Apparatus and methods of operation of passive LED lighting equipment", U.S. Patent application, 12/544545, Aug. 20, 2009.
[50] W. Chen and S. Y. R. Hui, "Elimination of electrolytic capacitor in an AC/DC light-emitting diode (LED) driver with high input power factor and constant output current," *IEEE Trans. Power Electron*, vol. 27, no. 3, pp. 1598–1607, Mar. 2012.
[51] R. A. Pinto, M. R. Cosetin, A. Campos, M. A. D. Costa, and R. N. D. Prado, "Compact emergency lamp using power LEDs," *IEEE Trans. Ind. Electron.*, vol. 59, no. 4, pp. 1728–1738, Apr. 2012.
[52] S. Y. R. Hui, S. N. Li, W. Chen, X. H. Tao, and W. M. Ng, "A novel passive LED drivers with long lifetime," *IEEE Trans. Power Electron.*, vol. 25, no. 10, pp. 2665–2672, Oct. 2010.
[53] A. Poppe, G. Farkas, V. Székely, Gy. Horváth, and M. Rencz, "Multi-domain simulation and measurement of power LED-s and power LED assemblies," in *Proc. 22nd IEEE Semicond. Thermal Meas. Manag. Symp.*, Dallas, TX, Mar. 2006, pp. 191–198.
[54] A. Poppe, G. Farkas, G. Molná, B. Katona, T. Temesvölgyi, and J. W. He, "Emerging standard for thermal testing of power LEDs and its possible implementation," *Proc. SPIE*, vol. 7784, pp. 38–52, Aug. 2010.
[55] G. Farkas, S. Haque, F. Wall, P. S. Martin, A. Poppe, Q. V. V. Vander, and G. Bognár, "Electric and thermal transient effects in high power optical devices," in *Proc. 20th IEEE Semicond. Thermal Meas. Manag. Symp.*, San Jose, CA, Mar. 2004, pp. 168–176.
[56] G. Farkas, A. Poppe, J. Schanda, and K. Muray, "Complex characterization of power LEDs: Simultaneous measurement of photometric/radiometric and thermal properties," in *Proc. CIE LED Conf.*, Tokyo, Japan, Mar. 2004, pp. 92–95.
[57] P. Pickard, "System architecture impacts on power supply design for solid state lighting,", presented at the IEEE Appl. Power Electronics Conf. Exhibition, Durham, NC, Feb. 2012, Industrial Session IS2.2.1.
[58] D. Cox, "System and power supply design considerations to address lifetime and cost goals for broad market acceptance of LED lighting applications", presented at the IEEE Application Power Electronics Conf. Exhibition, Durham, NC, Feb. 2012, Industrial Session IS2.2.3.

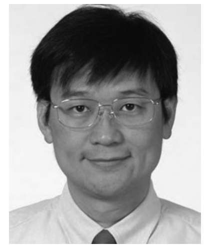

S. Y. R. Hui (F'03) received the B.Sc. (Eng.) degree (Hons.) from the University of Birmingham in 1984 and the D.I.C. and Ph.D. degrees from Imperial College London, London, U.K., in 1987.

He has previously held various academic positions at the University of Nottingham (1987–1990), the University of Technology, Sydney (1990–1991), the University of Sydney (1992–1996), and the City University of Hong Kong, Pokfulam, Hong Kong (1996–2011). Since July 2011, he has been holding the Chair Professorship at the University of Hong Kong. Since July 2010, he has also been concurrently holding the Chair Professorship of Power Electronics at Imperial College London. He has published more than 200 technical papers, including more than 160 refereed journal publications and book chapters. More than 50 of his patents have been adopted by industry.

Dr. Hui is a Fellow of the IET. He has been an Associate Editor of the IEEE TRANSACTIONS ON POWER ELECTRONICS since 1997 and an Associate Editor of the IEEE TRANSACTIONS ON INDUSTRIAL ELECTRONICS since 2007. He has been appointed twice as an IEEE Distinguished Lecturer by the IEEE Power Electronics Society in 2004 and 2006. He served as one of the 18 Administrative Committee members of the IEEE Power Electronics Society and was the Chairman of its Constitution and Bylaws Committee from 2002 to 2010. He received the Excellent Teaching Award at CityU in 1998 and the Earth Champion Award in 2008. He received the IEEE Best Paper Award from the IEEE IAS Committee on Production and Applications of Light in 2002, and two IEEE Power Electronics Transactions Prize Paper Awards for his publications on Wireless Battery Charging Platform Technology in 2009 and on LED system theory in 2010. His inventions on wireless charging platform technology underpin key dimensions of Qi, the world's first wireless power standard, with freedom of positioning and localized charging features for wireless charging of consumer electronics. In November 2010, he received the IEEE Rudolf Chope R&D Award from the IEEE Industrial Electronics Society, the IET Achievement Medal (The Crompton Medal), and was elected to the Fellowship of the Australian Academy of Technological Sciences and Engineering.

Huanting Chen was born in Zhangzhou, China, in 1982. He received the B.S. degree in physics from Zhangzhou Normal University, Zhangzhou, in 2005, and the Ph.D. degree in radio physics from Xiamen University, Xiamen, China, in 2010. He was a Joint Ph.D. Student at the Light and Lighting Laboratory, Catholic University College Gent, Belgium, from November 2009 to May 2010.

In September 2010, he became a Lecturer with the Department of Physics and Electronic Information Engineering, Zhangzhou Normal University. He is currently a Research Associate in the Department of Electrical and Electronic Engineering, The University of Hong Kong, China. His research interests include solid-state lighting technology and application.

Xuehui Tao was born in China. She received the B.S. degree in electronic science and technology and the M.S. degree in electronic engineering from Southwest Jiaotong University, Chengdu, China. She is currently working toward the Doctor of Philosophy degree at the Department of Electronic Engineering, City University of Hongkong, Kowloon, Hongkong, China.

Her current research interests include the design and development of switching-mode power supplies, LED driving circuits, electronic ballasts, and thermal management of LED and electronic components.